

Photoinduced  $\eta$ -pairing at finite temperaturesSatoshi Ejima<sup>1,2</sup>, Tatsuya Kaneko,<sup>3</sup> Florian Lange,<sup>1</sup> Seiji Yunoki,<sup>2,4,5</sup> and Holger Fehske<sup>1</sup><sup>1</sup>*Institute of Physics, University Greifswald, 17489 Greifswald, Germany*<sup>2</sup>*Computational Condensed Matter Physics Laboratory, RIKEN Cluster for Pioneering Research (CPR), Wako, Saitama 351-0198, Japan*<sup>3</sup>*Department of Physics, Columbia University, New York, New York 10027, USA*<sup>4</sup>*Computational Quantum Matter Research Team, RIKEN Center for Emergent Matter Science (CEMS), Wako, Saitama 351-0198, Japan*<sup>5</sup>*Computational Materials Science Research Team, RIKEN Center for Computational Science (R-CCS), Kobe, Hyogo 650-0047, Japan*

(Received 2 May 2020; accepted 24 June 2020; published 8 July 2020)

We numerically prove photoinduced  $\eta$ -pairing in a half-filled fermionic Hubbard chain at both zero and finite temperature. The result, obtained by combining the matrix-product-state based infinite time-evolving block decimation technique and the purification method, applies to the thermodynamic limit. Exciting the Mott insulator by a laser electric field docked on via the Peierls phase, we track the time evolution of the correlated many-body system and determine the optimal parameter set for which the nonlocal part of the  $\eta$ -pair-correlation function becomes dominant during the laser pump at zero and low temperatures. These correlations vanish at higher temperatures and long times after pulse irradiation. In the high laser frequency strong Coulomb coupling regime we observe a remnant enhancement of the Brillouin-zone boundary pair-correlation function also at high temperatures, if the Hubbard interaction is about a multiple of the laser frequency, which can be attributed to an enhanced double occupancy in the virtual Floquet state.

DOI: [10.1103/PhysRevResearch.2.032008](https://doi.org/10.1103/PhysRevResearch.2.032008)

**Introduction.** Optical pumping is not only an excellent tool to investigate complex few- and many-body systems but also makes it possible to create new phases of quantum matter with tunable properties [1–4]. Inducing superconductivity by light pulses in low-dimensional materials with strong electronic correlations is certainly one of the most fascinating options in this regard [5–7]. Thus, it was not surprising that a whole series of theoretical studies has addressed the microscopic modeling and understanding of this nonequilibrium light-matter-interaction phenomenon [8–12].

In this context, the so-called  $\eta$ -pairing, originally proposed by Yang for the Hubbard model [13], has attracted renewed attention [14–21]. Pumping the Mott insulating phase may result in an excited state with enhanced off-diagonal pair-density-wave correlations, which are absent in the ground state [15]. Here, the basic mechanism is the creation of  $\eta$ -pairs triggered by the nonlinear optical excitation of the system in conjunction with the selection rules. Interestingly, for low-amplitude pulses, the peak structure of the pair-correlation function is essentially the same as that obtained for the optical spectrum in the ground state, implying that the photoinduced state might indeed result from an  $\eta$ -pairing mechanism.

The crucial question is whether these findings will remain valid in the *thermodynamic limit* and at *finite temperature*  $T$ .

Some features, e.g., the stripe structure found in the structure factor of the pair correlations (Fig. 2 of Ref. [15]) of small systems, have been shown to disappear by increasing the system size [22], exploiting density-matrix renormalization group (DMRG) and time-evolving block decimation (TEBD) methods [23,24]. For sure, determining the temporal evolution of an *infinite, driven, strongly correlated* electron system at  $T > 0$  is one of the most difficult problems in solid state theory. Since the fermionic Hubbard model [25] can nowadays be realized in optical lattices [26–29], just as its bosonic counterpart [30], such a theoretical treatment is indispensable, however, for the interpretation of the experimental data, especially in one spatial dimension.

Despite this difficulty, this Rapid Communication aims at proving the existence of photoinduced  $\eta$ -pairing in the one-dimensional half-filled fermionic Hubbard model, directly in the thermodynamic limit and for finite temperatures. For this we exploit unbiased numerical techniques, specifically the infinite TEBD (iTEBD) technique [31] based on an infinite matrix-product-state (iMPS) representation [32] in combination with the purification method [33,34], which enables us to monitor the real-time evolution of thermal states at a finite target temperature, as accessible by optical-lattice experiments.

**Model.** Our starting point is the Hubbard Hamiltonian,

$$\hat{H} = -t_h \sum_{j,\sigma} (\hat{c}_{j,\sigma}^\dagger \hat{c}_{j+1,\sigma} + \text{H.c.}) + U \sum_j \left( \hat{n}_{j,\uparrow} - \frac{1}{2} \right) \left( \hat{n}_{j,\downarrow} - \frac{1}{2} \right), \quad (1)$$

Published by the American Physical Society under the terms of the [Creative Commons Attribution 4.0 International](https://creativecommons.org/licenses/by/4.0/) license. Further distribution of this work must maintain attribution to the author(s) and the published article's title, journal citation, and DOI.

where  $\hat{c}_{j,\sigma}^\dagger$  ( $\hat{c}_{j,\sigma}$ ) creates (annihilates) a fermion with spin projection  $\sigma$  ( $=\uparrow, \downarrow$ ) at lattice site  $j$ , and  $\hat{n}_{j,\sigma} = \hat{c}_{j,\sigma}^\dagger \hat{c}_{j,\sigma}$ . The first term represents the kinetic energy (with nearest-neighbor particle hopping amplitude  $t_h$ ) that acts against the Coulomb interaction (parametrized by the on-site Hubbard repulsion  $U$ ), which tends to localize the fermions by establishing a Mott insulating state at half band filling. The Hubbard Hamiltonian (1) commutes with the operator  $\hat{\eta}^2 = \frac{1}{2}(\hat{\eta}^+ \hat{\eta}^- + \hat{\eta}^- \hat{\eta}^+) + (\hat{\eta}^z)^2$ , where  $\hat{\eta}^z = \frac{1}{2} \sum_j (\hat{n}_{j,\uparrow} + \hat{n}_{j,\downarrow} - 1)$ ,  $\hat{\eta}^+ = \sum_j (-1)^j \hat{\Delta}_j^\dagger$ ,  $\hat{\eta}^- = (\hat{\eta}^+)^\dagger$ , and  $\hat{\Delta}_j^\dagger = \hat{c}_{j,\downarrow}^\dagger \hat{c}_{j,\uparrow}^\dagger$  denotes the on-site singlet pair creation operator (see Ref. [35]).

As demonstrated in Ref. [15], photoinduced  $\eta$ -pairing states may appear when an external time-dependent field couples to the hopping term via a Peierls phase [36],  $t_h \hat{c}_{j,\sigma}^\dagger \hat{c}_{j+1,\sigma} \rightarrow t_h e^{iA(t)} \hat{c}_{j,\sigma}^\dagger \hat{c}_{j+1,\sigma}$ , where the vector potential

$$A(t) = A_0 e^{-(t-t_0)^2/(2\sigma_p^2)} \cos[\omega_p(t-t_0)] \quad (2)$$

describes a pump pulse with amplitude  $A_0$ , frequency  $\omega_p$ , and width  $\sigma_p$ , centered at time  $t_0$  ( $>0$ ). As a result, the Hamiltonian becomes time dependent,  $\hat{H} \rightarrow \hat{H}(t)$ , and the initial (equilibrium) ground state evolves (forward) in time:  $|\psi(0)\rangle \rightarrow |\psi(t)\rangle$ . Numerically such a time evolution can be treated in an efficient manner by combining TEBD and second-order Suzuki-Trotter decomposition methods [24]. Hereafter we use  $t_h$  ( $t_h^{-1}$ ) as the unit of energy (time), and set the time step  $\delta t \cdot t_h = 0.01$ .

In fact, using the iTEBD technique, we directly examine the time evolution of the pair-correlation function,

$$P(r, t) = \frac{1}{L} \sum_j \langle \psi(t) | (\hat{\Delta}_{j+r}^\dagger \hat{\Delta}_j + \text{H.c.}) | \psi(t) \rangle, \quad (3)$$

in case that the number of lattice sites  $L \rightarrow \infty$ . At  $r=0$ , the pair correlation gives twice the number of double occupancy, i.e.,  $P(0, t) = 2n_d(t) = (2/L) \sum_j \langle \psi(t) | \hat{n}_{j,\uparrow} \hat{n}_{j,\downarrow} | \psi(t) \rangle$ . Most notably, the Fourier transform  $\tilde{P}(q, t) = \sum_r e^{iqr} P(r, t)$  shows an enhancement after the pulse irradiation that was believed to be indicative of  $\eta$ -pairing in finite Hubbard clusters [15]. Since we are particularly interested in longer-range pair correlations, we will also analyze the modified structure factor  $\tilde{P}_{r>0}(q, t) = \sum_{r>0} e^{iqr} P(r, t)$ , in which the contribution of the double occupancy  $n_d(t)$  is excluded. Let us point out that  $\tilde{P}(q, t)$  obtained by iTEBD in the iMPS representation fulfils the relation  $\tilde{P}(\pi, t) = 2 \langle \psi(t) | \hat{\eta}^+ \hat{\eta}^- | \psi(t) \rangle / L$ , which is not the case in any (finite-system) TEBD calculation with open boundary conditions (OBCs) (see Ref. [22] and the Supplemental Material [35]).

*iTEBD results at  $T=0$ .* In a first step, we determine the optimal parameter set in view of an enhancement of  $\tilde{P}(\pi, t)$  at zero temperature. Figures 1(a)–1(c) provide iTEBD contour plots for  $\tilde{P}(\pi, t)$ , in dependence on  $A_0$  and  $\omega_p$ , at different times  $t \cdot t_h$ . For  $t < t_0$ , in the ramp-up regime of the pump field, the spectral intensity of  $\tilde{P}(\pi, t)$  is negligibly small (not shown). Noticeable pair correlations develop for  $t \gtrsim t_0$ , albeit the signal is very broad [cf. Fig. 1(a)]. It becomes focused when the light pulse acts on the system [Fig. 1(b)], and reaches its saturation value for  $t \cdot t_h \simeq 16$  [Fig. 1(c)], where  $A_0 = 0.37$  and  $\omega_p = 7.10$ .

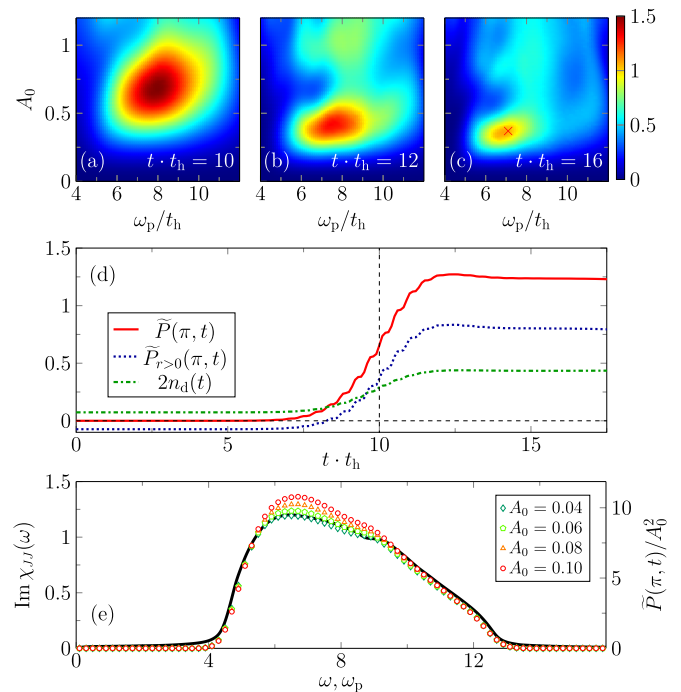


FIG. 1. Time evolution of pair correlations in an infinite half-filled Hubbard chain at  $T=0$ . Contour plots of  $\tilde{P}(\pi, t)$  are given in the  $\omega_p$ - $A_0$  plane at  $t \cdot t_h = 10$  (a), 12 (b), and 16 (c) for  $U/t_h = 8$ , where the pump is parametrized by  $\sigma_p = 2$  at  $t_0 \cdot t_h = 10$ .  $\tilde{P}(\pi, t)$ ,  $\tilde{P}_{r>0}(\pi, t)$ , and  $2n_d(t)$  are displayed as functions of time in (d) for the peak position  $\times$  read off from (c). (e) demonstrates that the  $\tilde{P}(\pi, t)/A_0^2$  data at  $t \cdot t_h = 16$  (symbols) can be rescaled to  $\text{Im } \chi(\omega)$  (black line) for small  $A_0$ , where  $\text{Im } \chi(\omega)$  is the imaginary part of the optical spectrum  $\chi_{JJ}(\omega)$ . iTEBD data were obtained with bond dimensions up to  $\chi = 2000$ . For a discussion of the accuracy of the iTEBD calculations, see the Supplemental Material [35].

Figure 1(d) relates the time evolution of  $\tilde{P}(\pi, t)$ ,  $\tilde{P}_{r>0}(\pi, t)$ , and  $2n_d(t)$  for the optimal parameter set marked by a cross in Fig. 1(c). All quantities show a clear response to pulse irradiation and will be strengthened as the system progresses in time until saturation is reached. Apparently, here, the nonlocal contributions  $\tilde{P}_{r>0}(\pi, t)$  have a stronger impact on  $\tilde{P}(\pi, t)$  than double occupancy.

A notable finding of previous ED calculations [15] was a peak structure of  $\tilde{P}(\pi, t)$  as a function of  $\omega_p$  which is essentially the same—for small  $A_0$ —as those of the ground-state optical spectrum  $\chi_{JJ}(\omega)$ , folded with an appropriate Lorentzian of width  $\eta_L$  (depending on  $1/\sigma_p$ ). The current-current spectral function  $\chi_{JJ}(\omega)$  is given by

$$\chi_{JJ}(\omega > 0) = -\frac{1}{L} \langle \psi_0 | \hat{J} \frac{1}{E_0 - \hat{H} + \hbar\omega + i\eta_L} \hat{J} | \psi_0 \rangle, \quad (4)$$

where  $|\psi_0\rangle$  is the ground state having energy  $E_0$ , and the charge current operator  $\hat{J}$ , for the Hubbard model, takes the form  $\hat{J} = it_h \sum_{\sigma\ell} (\hat{c}_{\ell,\sigma}^\dagger \hat{c}_{\ell+1,\sigma} - \hat{c}_{\ell+1,\sigma}^\dagger \hat{c}_{\ell,\sigma})$ . The ED [15] and TEBD [22] calculations, which could be conducted for small lattices only, suffer from finite-size effects however. These give rise, *inter alia*, to stripe patterns in  $\tilde{P}(\pi, t)$ , which makes it difficult to determine its maximum value. We demonstrate that a single peak structure evolves in the thermodynamic

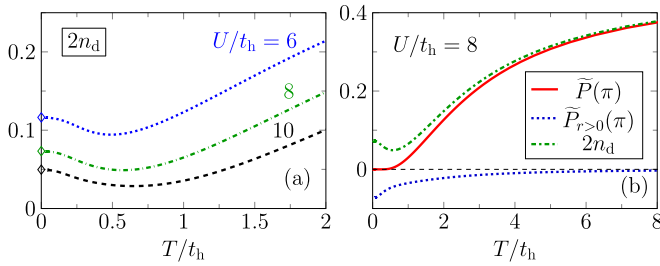


FIG. 2. Temperature dependence of various correlation functions for the half-filled Hubbard chain without irradiation. Double occupancy  $n_d$  at different Coulomb repulsions  $U/t_h$  (a) [here, the symbols mark data obtained by a separate ground-state simulation ( $T = 0$ )] and pair correlators  $\tilde{P}(\pi)$ ,  $\tilde{P}_{r>0}(\pi)$  compared to  $n_d$  for  $U/t_h = 8$  (b).

limit  $L \rightarrow \infty$  [see Fig. 1(c)], and therefore can address more seriously the question whether the  $\chi_{JJ}(\omega)$  line shape obtained by time-dependent iMPS-based DMRG really agrees with that of  $\tilde{P}(\pi, t)$  for small  $A_0$  and large  $t$ , where  $\tilde{P}(\pi)$  becomes time independent.

Figure 1(e) compares the iTEBD data, obtained for  $\tilde{P}(\pi, t)$  at various small  $A_0$  and  $t \cdot t_h = 16$ , with the DMRG results for  $\chi_{JJ}(\omega)$  (using  $\eta_L/t_h = 0.2$ ), in dependence on  $\omega_p$  respectively  $\omega$ . Here, we show that  $\tilde{P}(\pi, t)$  divided by  $A_0^2$  scales to the imaginary part of the optical spectrum  $\text{Im} \chi(\omega)$  [ $\simeq \tilde{P}(\pi, t)/CA_0^2$  with  $C \sim 7.9$ ] since the double occupancy  $n_d$  is proportional to  $A_0^2$ , for very small  $A_0^2$ , in a wide  $\omega_p$ -range around the resonant frequency  $\omega_p \simeq U$  [37]. Close to the maximum in  $\tilde{P}$  respectively  $\text{Im} \chi$ , at about  $\omega \simeq 6.49$ , both quantities differ for larger amplitudes  $A_0$ , because the nonlocal correlations contained in  $\tilde{P}_{r>0}(\pi, t)$  become increasingly important. Taking the relation  $\text{Im} \chi_{JJ}(\omega) = \omega \sigma_1(\omega)$  into account, where  $\sigma_1(\omega)$  is the real part of the optical conductivity, this behavior is in accordance with DMRG and field-theory results for the optical response in the half-filled Hubbard model [38].

*iTEBD results for  $T > 0$ .* In a second step, we will investigate—under usage of the iMPS and purification approaches [33,34]—what happened to the  $\eta$ -pairing correlations at finite temperatures  $T = 1/\beta$ . Methodically, to obtain the equilibrium state  $|\psi_T\rangle$  at some target temperature  $T$ , we first construct an iMPS representation of a state  $|\psi_\infty\rangle$  at infinite temperature, where each physical site is in a maximally entangled state with an auxiliary site, and then carry out the imaginary-time evolution  $e^{-\beta \hat{H}/2} |\psi_\infty\rangle$  of the physical system. We note that combining the Suzuki-Trotter decomposition with swap gates [39], such a time evolution can be effectively implemented for any nearest-neighbor Hamiltonian.

We start by checking the temperature dependence of the double occupancy  $n_d$  in the pure Hubbard model (1) without an optical pump. Our iTEBD data in Fig. 2(a) reveal the well-known minimum in  $n_d$  [40], which is shifted to higher temperatures as  $U$  increases and is related to the maximum in the local magnetic moment  $L_0 = \frac{3}{4} \langle (n_{j,\uparrow} - n_{j,\downarrow})^2 \rangle$  [ $= \frac{3}{4}(1 - 2n_d)$  at half filling]. At  $T = 0$ ,  $L_0$  interpolates between the atomic limit ( $U = \infty$ ) with  $L_0 = 3/4$  since  $n_d = 0$  and the band limit ( $U = 0$ ) where  $L_0 = 3/8$ , i.e.,  $n_d = 1/4$ , which is also the value for  $T \rightarrow \infty$  since empty, spin-up/down, and double occupied sites are equally likely. Figure 2(b) shows

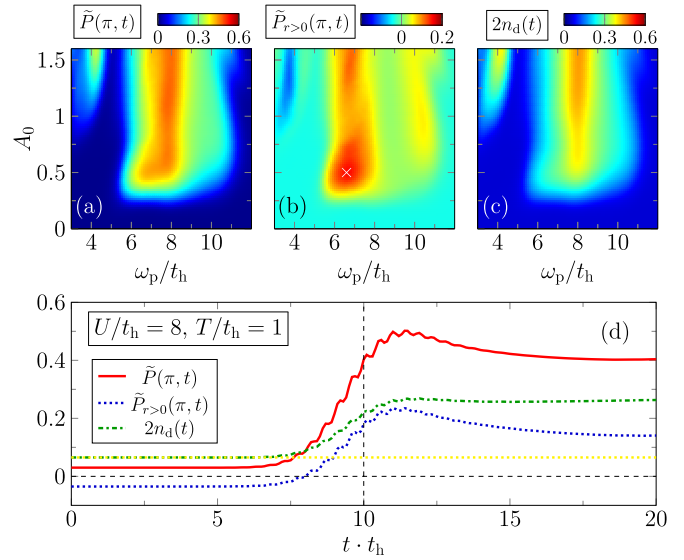


FIG. 3. Pair correlations in an infinite half-filled Hubbard chain at  $T > 0$ . Contour plots of  $\tilde{P}(\pi, t)$  (a),  $\tilde{P}_{r>0}(\pi, t)$  (b), and  $2n_d(t)$  (c) in the  $\omega_p$ - $A_0$  plane at time  $t \cdot t_h = 20$  for  $T/t_h = 1$ , after pulse irradiation where  $\sigma_p = 2$ ,  $t_0 \cdot t_h = 10$ , and  $U/t_h = 8$ , obtained by iTEBD with bond dimensions  $\chi = 800$ . Time evolution of  $\tilde{P}(\pi, t)$ ,  $\tilde{P}_{r>0}(\pi, t)$ , and  $2n_d(t)$  (d) for parameters corresponding to the peak position  $\times$  in (b). The dotted yellow line marks  $2n_d(t = 0)$  for the pure Hubbard model with corresponding parameters. The iTEBD data are obtained for bond dimension  $\chi = 1600$ .

the temperature dependence of  $\tilde{P}(\pi)$ , together with those of  $\tilde{P}_{r>0}(\pi)$  and  $n_d$ . At  $T = 0$ , on-site ( $n_d$ ) and nonlocal [ $\tilde{P}_{r>0}(\pi)$ ] contributions cancel each other, so that  $\tilde{P}(\pi) = 0$ . Clearly the pairing correlations vanish in the opposite  $T \rightarrow \infty$ , expressed by the fact that  $\tilde{P}_{r>0}(\pi) \rightarrow 0$  and the  $\tilde{P}(\pi)$  curve tends to  $2n_d$  (see also Ref. [20]). As a result, strong  $\eta$ -pair correlations can be expected in the low-temperature region at best.

Now, we take into consideration a time-dependent external field and carry out the real-time evolution of  $\hat{H}(t)$  to a thermal equilibrium state  $|\psi_T\rangle$ . This allows us to discuss the development of  $\eta$ -pairing correlations as a function of time at  $T > 0$ . Figures 3(a)–3(c) provide iTEBD contour plots of  $\tilde{P}(q = \pi, t)$ ,  $\tilde{P}(q = \pi, t)$ , and  $2n_d(t)$  in the  $\omega_p$ - $A_0$  plane for  $T/t_h = 1.0$ , at  $t \cdot t_h = 20$ , following the pulse exposure. We find a persistent enhancement of  $\tilde{P}(\pi, t)$ . The crucial question is whether this enhancement can be related to the nonlocal part of the pairing-correlation function, or simply stems from the on-site (double-occupancy) contribution to  $P(r, t)$ . The answer can be read off from the contour plot of  $\tilde{P}_{r>0}(\pi, t)$  [Fig. 3(b)], which demonstrates its noticeable contribution. Figure 3(c) gives the corresponding values of double occupancy  $2n_d(t)$ . Here, we find two maxima at about  $\omega_p \sim U$  and  $2\omega_p \sim U$  which can be assigned to resonant driving, i.e., to the existence of a Floquet virtual state [41]. How  $\tilde{P}_{r>0}(\pi, t)$  and  $2n_d(t)$  will influence  $\tilde{P}(q = \pi, t)$  over time can be seen in more detail in Fig. 3(d) for  $\omega_p/t_h = 6.6$  and  $A_0 = 0.5$  [ $\times$  position in Fig. 3(c)]. Apparently, all these quantities are growing when the light pulse acts on the correlated system [around  $t_0 \cdot t_h (=10)$ ]. Here, the (photoinduced) nonequilibrium physics emerges. Note that the line

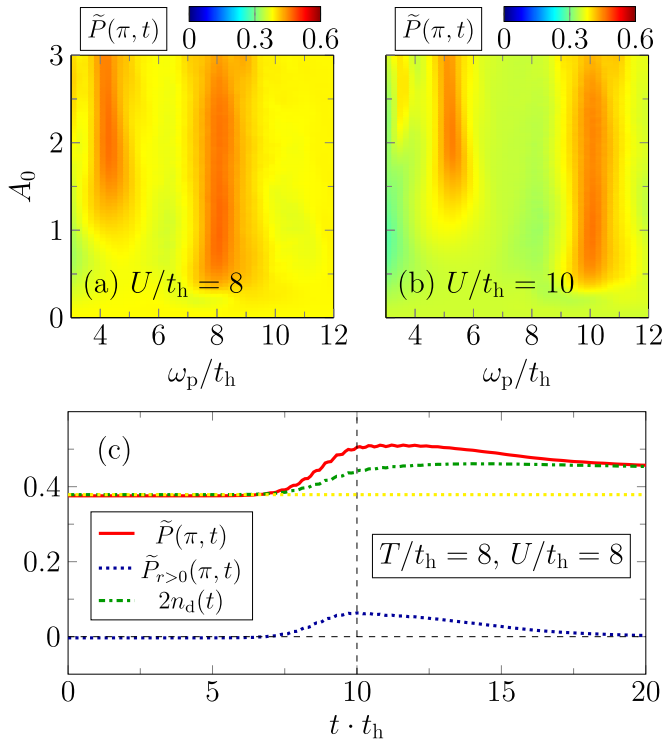


FIG. 4. Pair correlations at high temperatures. Contour plots of  $\tilde{P}(\pi, t)$  at  $T/t_h = 8$ , calculated for  $U/t_h = 8$  (a) and 10 (b) by iTEBD with  $\chi = 800$ , where the pump is parametrized as before. Time evolution of  $\tilde{P}(\pi, t)$ ,  $\tilde{P}_{r>0}(\pi, t)$ , and  $2n_d(t)$  (c), for the peak-position parameters determined from  $\tilde{P}_{r>0}(\pi, t \cdot t_h = 15)$  [see Fig. S2(d) in the Supplemental Material [35]] by iTEBD with  $\chi = 1600$ .

shape of  $\tilde{P}(\pi, t)$  (and especially its decay at larger times) is largely determined by  $\tilde{P}_{r>0}(\pi, t)$ . At  $t \cdot t_h \gtrsim 20$  saturation is reached. The comparison with the pure Hubbard model results shows the predicted dynamical generation of double occupancy [42,43] after pulse irradiation.

Finally, we look at the system response to the pulse at higher temperatures ( $T \sim U$ ). Figures 4(a) and 4(b) display the contour plots of  $\tilde{P}(\pi, t)$ , after pumping ( $t \cdot t_h = 20$ ), for  $U/t_h = 8$  and  $U/t_h = 10$ , respectively. Again we observe pronounced maxima when the pulse frequency is close to  $\omega_p \simeq U/m$ , which comes to light for  $m = 1, 2$  in Fig. 4(a) and  $m = 1, 2, 3$  in Fig. 4(b). Figure 4(c) elucidates the origin of this multippeak structure and the significant differences to the behavior at low temperatures shown in Fig. 3(d). Before pulse irradiation and at long times [where  $\tilde{P}(\pi, t)$  reaches its saturation value],  $\tilde{P}(\pi, t)$  is completely determined by

$2n_d(t)$ . The pure Hubbard model result is maintained up to  $t \cdot t_h \simeq 7.5$  (cf. the dotted line), which can be considered as the linear response regime [41]. The nonequilibrium dynamics is evidenced at intermediate times  $7 \lesssim t \cdot t_h \lesssim 13$ , when the irradiation is strong. In contrast to low temperatures, the contribution of  $\tilde{P}_{r>0}(\pi, t)$  is negligible after pulse irradiation for  $t \cdot t_h \gtrsim 18$ . This shows that the peak structure observed in Figs. 4(a) and 4(b) can be attributed to the enhanced double occupancy. The high-frequency expansion in the Floquet picture reveals the underlying mechanism: Performing a Schrieffer-Wolff transformation [44,45] for a periodically driven Hubbard model in the strong-coupling regime, an effective (Heisenberg) Hamiltonian is obtained (see, e.g., Ref. [46]), containing an effective exchange interaction  $J_{\text{eff}}$ , which diverges at the resonant frequencies  $U \simeq m\omega_p$  [47]. Since time periodicity  $\hat{H}(t + \tau) = \hat{H}(t)$  with  $\tau = 2\pi/\omega_p$  is absent in our model (1) and (2), the photoinduced double occupancy appears as a Floquet virtual state as in the nonequilibrium dynamics of pumped Mott insulators [41]. This effect can be observed at any temperature [see, e.g., Fig. 3(c)].

**Conclusions.** To sum up, we have demonstrated light-pulse photoinduced  $\eta$ -pairing in the one-dimensional half-filled Hubbard model at both zero and finite temperatures by means of a *de facto* approximation-free numerical approach. For zero temperature, we carved out finite-size effects of previous exact diagonalization studies, but confirmed the basic relation between the pair-correlation function and the ground-state optical spectrum for the infinite system. With a view to experiments, also the optimal pulse for an enforcement of  $\eta$ -pair correlations  $\tilde{P}(\pi, t)$  is determined. For finite but low temperatures, nonlocal pairing correlations  $\tilde{P}_{r>0}(\pi, t)$  were detected within the applied iTEBD-purification scheme. After pulse irradiation a dynamical generation of double occupancy is proved for finite temperatures. Overall, our results support a scenario where optical excitation of a Mott insulator may lead to a (nonequilibrium) state with very slowly decaying pairing correlations. If fermionic optical lattices will be cooled to temperatures  $T \lesssim J_{\text{ex}} = 4t_h^2/U < t_h$  in the strong-coupling regime ( $U \gg t_h$ ) [29], our findings should be detected in the laboratory.

**Acknowledgments.** The iTEBD simulations were performed using the ITensor library [48]. S.E. and F.L. were supported by Deutsche Forschungsgemeinschaft through Projects No. EJ 7/2-1 and No. FE 398/10-1, respectively. T.K. acknowledges support from the JSPS Overseas Research Fellowship. S.Y. was supported in part by Grants-in-Aid for Scientific Research from JSPS (Project No. JP18H01183) of Japan.

- [1] H. Ichikawa, S. Nozawa, T. Sato, A. Tomita, K. Ichiyangi, M. Chollet, L. Guerin, N. Dean, A. Cavalleri, S.-i Adachi, T.-h. Arima, H. Sawa, Y. Ogimoto, M. Nakamura, R. Tamaki, K. Miyano, and S.-y. Koshihara, *Nat. Mater.* **10**, 101 (2011).  
 [2] D. N. Basov, R. D. Averitt, and D. Hsieh, *Nat. Mater.* **16**, 1077 (2017).

- [3] S. Mor, M. Herzog, D. Golež, P. Werner, M. Eckstein, N. Katayama, M. Nohara, H. Takagi, T. Mizokawa, C. Monney, and J. Stähler, *Phys. Rev. Lett.* **119**, 086401 (2017).  
 [4] S. Ishihara, *J. Phys. Soc. Jpn.* **88**, 072001 (2019).  
 [5] D. Fausti, R. I. Tobey, N. Dean, S. Kaiser, A. Dienst, M. C. Hoffmann, S. Pyon, T. Takayama, H. Takagi, and A. Cavalleri, *Science* **331**, 189 (2011).

- [6] W. Hu, S. Kaiser, D. Nicoletti, C. R. Hunt, I. Gierz, M. C. Hoffmann, M. L. Tacon, T. Loew, B. Keimer, and A. Cavalleri, *Nat. Mater.* **13**, 705 (2014).
- [7] M. Mitrano, A. Cantaluppi, D. Nicoletti, S. Kaiser, A. Perucchi, S. Lupi, P. Di Pietro, D. Pontiroli, M. Riccò, S. R. Clark, D. Jaksch, and A. Cavalleri, *Nature (London)* **530**, 461 (2016).
- [8] M. A. Sentef, A. F. Kemper, A. Georges, and C. Kollath, *Phys. Rev. B* **93**, 144506 (2016).
- [9] M. Knap, M. Babadi, G. Refael, I. Martin, and E. Demler, *Phys. Rev. B* **94**, 214504 (2016).
- [10] D. M. Kennes, E. Y. Wilner, D. R. Reichman, and A. J. Millis, *Nat. Phys.* **13**, 479 (2017).
- [11] Y. Murakami, N. Tsuji, M. Eckstein, and P. Werner, *Phys. Rev. B* **96**, 045125 (2017).
- [12] G. Mazza and A. Georges, *Phys. Rev. B* **96**, 064515 (2017).
- [13] C. N. Yang, *Phys. Rev. Lett.* **63**, 2144 (1989).
- [14] S. Kitamura and H. Aoki, *Phys. Rev. B* **94**, 174503 (2016).
- [15] T. Kaneko, T. Shirakawa, S. Sorella, and S. Yunoki, *Phys. Rev. Lett.* **122**, 077002 (2019).
- [16] J. Tindall, B. Buča, J. R. Coulthard, and D. Jaksch, *Phys. Rev. Lett.* **123**, 030603 (2019).
- [17] R. Fujiuchi, T. Kaneko, Y. Ohta, and S. Yunoki, *Phys. Rev. B* **100**, 045121 (2019).
- [18] F. Peronaci, O. Parcollet, and M. Schiró, *Phys. Rev. B* **101**, 161101(R) (2020).
- [19] J. Li, D. Golez, P. Werner, and M. Eckstein, *arXiv:1908.08693*.
- [20] T. Kaneko, S. Yunoki, and A. J. Millis, *arXiv:1910.11229*.
- [21] R. Fujiuchi, T. Kaneko, K. Sugimoto, S. Yunoki, and Y. Ohta, *Phys. Rev. B* **101**, 235122 (2020).
- [22] S. Ejima, T. Kaneko, F. Lange, S. Yunoki, and H. Fehske, *JPS Conf. Proc.* **30**, 011184 (2020).
- [23] S. R. White, *Phys. Rev. Lett.* **69**, 2863 (1992).
- [24] G. Vidal, *Phys. Rev. Lett.* **91**, 147902 (2003).
- [25] J. Hubbard, *Proc. R. Soc. London, Ser. A* **276**, 238 (1963).
- [26] D. Jaksch and P. Zoller, *Ann. Phys.* **315**, 52 (2005).
- [27] M. Lewenstein, A. Sanpera, V. Ahufinger, B. Damski, A. Sen(De), and U. Sen, *Adv. Phys.* **56**, 243 (2007).
- [28] U. Schneider, L. Hackermüller, J. P. Ronzheimer, S. Will, S. Braun, T. Best, I. Bloch, E. Demler, S. Mandt, D. Rasch, and A. Rosch, *Nat. Phys.* **8**, 213 (2012).
- [29] A. Mazurenko, C. S. Chiu, G. Ji, M. F. Parsons, M. Kanász-Nagy, R. Schmidt, F. Grusdt, E. Demler, D. Greif, and M. Greiner, *Nature (London)* **545**, 462 (2017).
- [30] H. A. Gersch and G. C. Knollman, *Phys. Rev.* **129**, 959 (1963).
- [31] G. Vidal, *Phys. Rev. Lett.* **98**, 070201 (2007).
- [32] U. Schollwöck, *Ann. Phys.* **326**, 96 (2011).
- [33] M. Suzuki, *J. Phys. Soc. Jpn.* **54**, 4483 (1985).
- [34] F. Verstraete, J. J. García-Ripoll, and J. I. Cirac, *Phys. Rev. Lett.* **93**, 207204 (2004).
- [35] See Supplemental Material at <http://link.aps.org/supplemental/10.1103/PhysRevResearch.2.032008> for details, which includes Ref. [49].
- [36] R. Peierls, *Z. Phys.* **80**, 763 (1933).
- [37] T. Oka, *Phys. Rev. B* **86**, 075148 (2012).
- [38] E. Jeckelmann, F. Gebhard, and F. H. L. Essler, *Phys. Rev. Lett.* **85**, 3910 (2000).
- [39] E. M. Stoudenmire and S. R. White, *New J. Phys.* **12**, 055026 (2010).
- [40] H. Fehske and B. Lorenz, *J. Phys. C: Solid State Phys.* **17**, 5031 (1984).
- [41] Y. Wang, M. Claassen, B. Moritz, and T. P. Devereaux, *Phys. Rev. B* **96**, 235142 (2017).
- [42] S. D. Huber and A. Rüegg, *Phys. Rev. Lett.* **102**, 065301 (2009).
- [43] M. Messer, K. Sandholzer, F. Görg, J. Minguzzi, R. Desbuquois, and T. Esslinger, *Phys. Rev. Lett.* **121**, 233603 (2018).
- [44] S. Rahav, I. Gilyar, and S. Fishman, *Phys. Rev. A* **68**, 013820 (2003).
- [45] M. Bukov, M. Kolodrubetz, and A. Polkovnikov, *Phys. Rev. Lett.* **116**, 125301 (2016).
- [46] T. Oka and S. Kitamura, *Annu. Rev. Condens. Matter Phys.* **10**, 387 (2019).
- [47] A. Herrmann, Y. Murakami, M. Eckstein, and P. Werner, *Europhys. Lett.* **120**, 57001 (2017).
- [48] <http://itensor.org/>.
- [49] F. H. L. Essler, H. Frahm, F. Göhmann, A. Klümper, and V. E. Korepin, *The One-Dimensional Hubbard Model* (Cambridge University Press, Cambridge, UK, 2005).